The Plant Cell, Vol. 11, 1217–1226, July 1999, www.plantcell.org © 1999 American Society of Plant Physiologists

ANTHOCYANINLESS2, a Homeobox Gene Affecting Anthocyanin Distribution and Root Development in Arabidopsis

Hiroyoshi Kubo,[a,1,2] Anton J. M. Peeters,[b,1] Mark G. M. Aarts,[c] Andy Pereira,[c] and Maarten Koornneef[b]

[a] Department of Biology, Faculty of Science, Shinshu University, Matsumoto 390-8621, Japan
[b] Laboratory of Genetics, Wageningen Agricultural University, Dreijenlaan 2, 6703 HA Wageningen, The Netherlands
[c] Department of Molecular Biology, DLO-Centre for Plant Breeding and Reproduction Research (CPRO-DLO), Postbus 16, 6700 AA Wageningen, The Netherlands

The *ANTHOCYANINLESS2* (*ANL2*) gene was isolated from Arabidopsis by using the maize *Enhancer–Inhibitor* transposon tagging system. Sequencing of the *ANL2* gene showed that it encodes a homeodomain protein belonging to the HD–GLABRA2 group. As we report here, this homeobox gene is involved in the accumulation of anthocyanin and in root development. Histological observations of the *anl2* mutant revealed that the accumulation of anthocyanin was greatly suppressed in subepidermal cells but only slightly reduced in epidermal cells. Furthermore, the primary roots of the *anl2* mutant showed an aberrant cellular organization. We discuss a possible role of ANL2 in the accumulation of anthocyanin and cellular organization of the primary root.

INTRODUCTION

Anthocyanins are plant pigments that are responsible for a variety of red, blue, and purple colors. Anthocyanin accumulation occurs in certain plant tissues at specific developmental stages and is subject to control by many environmental factors, such as light, temperature, nutrients, and stress (Blank, 1958; Beggs and Wellmann, 1994). Most enzymes involved in anthocyanin biosynthesis are well characterized, and the structures of the corresponding genes have been determined for many plant species. Several regulatory genes for anthocyanin biosynthesis already have been identified in various plants (Dooner and Robbins, 1991). For example, the maize *R*/*B* gene family shows sequence similarity to *MYC* oncogenes. The *R* and *B* loci regulate the tissue specificity of anthocyanin biosynthesis in combination with another gene family, *C1*/*Pl*, whose members play a role in light regulation of the pathway and are related to *MYB* oncogenes. Moreover, the *Delila* gene of Antirrhinum encodes a transcription factor closely related to the *R* gene family in maize (Goodrich et al., 1992), and *Eluta* and *Rosea* control the pattern of anthocyanin production in Antirrhinum flowers (Martin et al., 1991; Martin and Gerats, 1993). In petunia, the regulatory genes *AN1*, *AN2*, and *AN11* have been cloned. *AN1* and *AN2* encode MYC- and MYB-type transcription factors, respectively (Mol et al., 1996). *AN11* encodes another type of regulatory protein containing a WD40 repeat motif (de Vetten et al., 1997). Although much research has been done, the mechanisms that control the spatial and temporal regulation of anthocyanin accumulation have not been elucidated.

In Arabidopsis, several mutants lacking anthocyanin have been isolated (Koornneef, 1990). These *transparent testa* (*tt*) mutants produce yellow or pale brown seeds because they lack brown pigment in the seed coat. *TT3*, *TT4*, and *TT5* have been found to encode dihydroflavonol-4-reductase (DFR), chalcone synthase (CHS), and chalcone flavanone isomerase (CHI), respectively (Shirley et al., 1992). *TTG* and *TT8* are regulatory genes that control transcription of DFR but not CHS and CHI (Shirley et al., 1995). The *ttg* mutant lacks not only anthocyanin but trichomes. The *ttg* mutant is restored to the wild type when transformed with the maize *R* gene (Lloyd et al., 1992).

Homeobox genes are another universal group of regulatory genes; however, they have not been associated with anthocyanin biosynthesis. The many homeodomain proteins that have been found in higher plants are divided into five groups: HD–KNOTTED1, HD–BELL1, homeodomain leucine zipper protein (HD–ZIP), plant homeodomain finger protein (PHD–Finger), and HD–GLABRA2 (GL2) (Lu et al., 1996). Recent research has shown that in general, homeobox genes play a role in cell specification and pattern formation in higher plants. *KNOTTED1* and *SHOOT MERISTEMLESS* are considered to be involved in maintaining the indeterminate state of apical meristems (Long et al., 1996; Kerstetter et al.,

[1] These authors contributed equally to this work.
[2] To whom correspondence should be addressed. E-mail hkubo77@gipac.shinshu-u.ac.jp; fax 81-263-37-2560.

1997). *BELL1* is required for integument development (Reiser et al., 1995). *Athb-8*, which encodes a protein belonging to the HD–ZIP group, is suggested to regulate vascular development (Baima et al., 1995). *GL2* regulates trichome development and suppresses root hair formation (Rerie et al., 1994). *ATML1* (for *Arabidopsis thaliana* meristem L1 layer), which encodes a protein belonging to the HD–GL2 group, is specifically expressed in the L1 layer of the vegetative shoot meristem and the inflorescence meristem. *ATML1* is suggested to be involved in setting up morphogenetic boundaries of positional information necessary for controlling cell specification and pattern formation (Lu et al., 1996).

Here, we report the isolation of another homeobox gene that encodes a protein belonging to the HD–GL2 group. This gene controls the anthocyanin pigmentation of the leaf subepidermal layer and cellular organization of the primary root.

RESULTS

Genetic Analysis

Heterologous tagging systems that use the maize transposon *Enhancer* (*En*)–*Inhibitor* (*I*) or *Activator–Dissociation* system have been used successfully in Arabidopsis (Aarts et al., 1993; Bancroft et al., 1993). In an Arabidopsis line containing the *En–I* system, we isolated a mutant with strong leaf anthocyanin variegation. This mutant produced normal brown seeds and was therefore different from *tt* and *ttg* mutants. We previously isolated an ethyl methanesulfonate–induced anthocyaninless mutant, called *anl1*, that is not allelic to this new mutant, which we called *anl2*. The *anl2* mutant showed variegation, indicating a high somatic transposon excision frequency. By backcrossing to Landsberg *erecta* (L*er*) plants, we were able to separate the transposon from the transposase source, thus stabilizing the transposon inserted in *anl2*. This also reduced the number of *I* elements present in the genome and facilitated further analysis of the mutant.

Pattern of Anthocyanin Accumulation

Under our growth conditions, rosette leaves of L*er* plants accumulate much anthocyanin (Figure 1A). This is in contrast to the stable *anl2* mutant, in which anthocyanin accumulation is reduced (Figure 1B). The unstable mutants showed variegation of anthocyanin pigmentation (Figure 1C). Variegation was observed only on the adaxial side of rosette leaves, whereas anthocyanin accumulated uniformly on the abaxial side of the leaves (Figures 1D and 1E). Furthermore, anthocyanin content on the adaxial side of rosette leaves of the stable mutant was greatly reduced, although there was also a slight reduction in anthocyanin content on the abaxial side (Figure 2). Cross-sections of rosette leaves were analyzed to determine the precise distribution of anthocyanin accumulation in leaves (Figures 1F and 1G). In the rosette leaves of L*er*, anthocyanin was observed to accumulate in subepidermal tissue of the adaxial side but in the epidermis of the abaxial side. In the *anl2* mutant, anthocyanin mainly accumulated in the epidermis of the abaxial side. These observations suggest that *ANL2* is a regulator of anthocyanin accumulation in subepidermal tissues.

To verify this possibility, we examined the accumulation of anthocyanin in other parts of the *anl2* mutant (Table 1). The

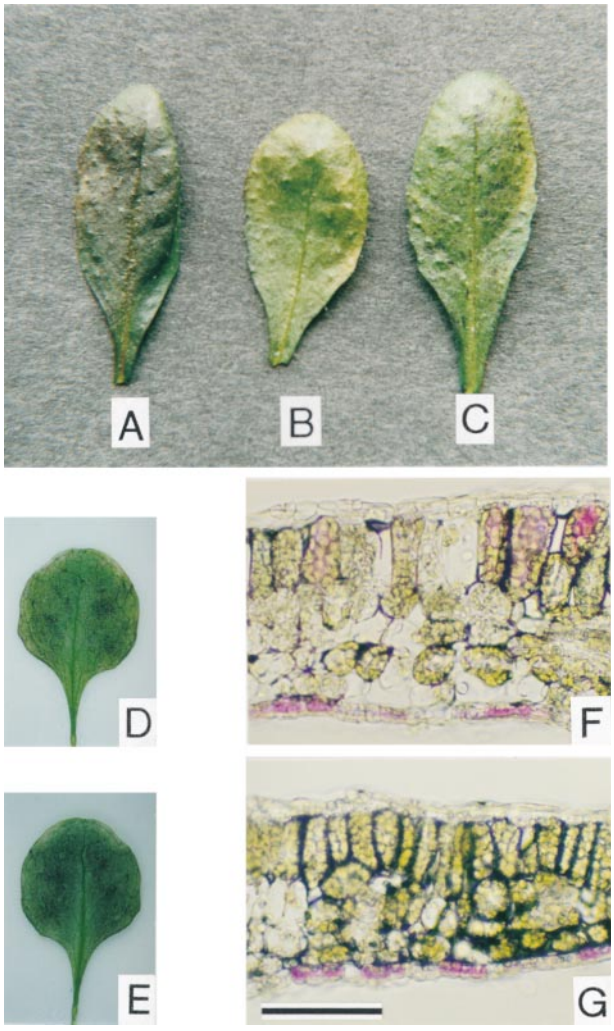

Figure 1. Pattern of Anthocyanin Accumulation in an *anl2* Mutant and a L*er* Plant.

(A) to **(C)** Adaxial side of rosette leaves from L*er*, a stable *anl2* mutant, and an unstable *anl2* mutant showing anthocyanin variegation, respectively.

(D) and **(E)** Upper and lower surfaces, respectively, of a rosette leaf showing variegation.

(F) and **(G)** Cross-sections of leaves from a L*er* plant and an *anl2* mutant, respectively. Bar in **(G)** = 100 μm for **(F)** and **(G)**.

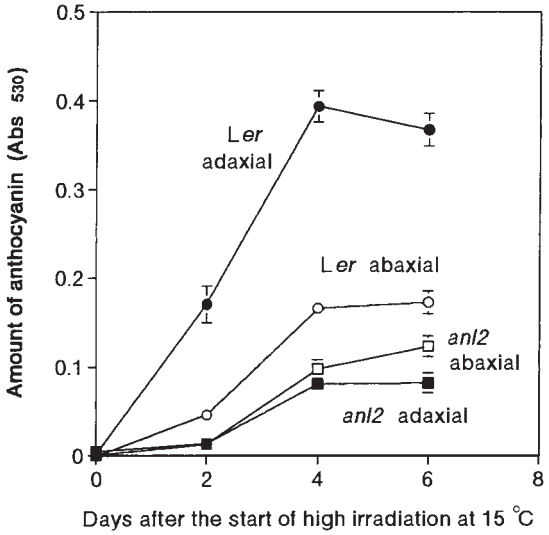

Figure 2. Time Course of Anthocyanin Accumulation in Rosette Leaves.

Time courses of anthocyanin accumulation were examined from the adaxial (filled circles and squares) and abaxial (open circles and squares) sides of rosette leaves from L*er* (filled and open circles) and *anl2* (filled and open squares) plants. Plants grown for 3 weeks at 22°C (7 W m^{-2}) were exposed to 15°C (11 W m^{-2}) for 0 to 6 days to induce anthocyanin accumulation. Anthocyanin was extracted from each layer (adaxial and abaxial sides) of a rosette leaf separately. The amount of anthocyanin was expressed as absorbance (Abs) at 530 nm per leaf area. The average of 10 rosette leaves is shown. Error bars indicate ±SE.

seedlings of the *anl2* mutant accumulated less anthocyanin than did the seedlings of L*er*. Anthocyanin was greatly reduced in all organs in which anthocyanin normally accumulates in subepidermal tissue (i.e., the adaxial side of leaves, stems, and flower buds), in contrast to the abaxial side of the rosette leaf. The *banyuls* (*ban*) mutant is known to accumulate high levels of anthocyanins in the most internal layer of the seed coat, which is derived from the L1 layer of the meristem (Albert et al., 1997). To examine whether the anthocyanin level in the L1-derived tissue was influenced in the *anl2* mutant, we examined anthocyanin accumulation in an *anl2 ban* double mutant. The *anl2 ban* double mutant accumulated amounts of anthocyanin similar to those accumulated by the monogenic *ban* mutant (Table 1). This means that *ANL2* is not required for anthocyanin accumulation in the internal layer of the seed coat, which is derived from the L1 layer of the meristem.

Cloning and Genetic Mapping of *ANL2*

To isolate the *ANL2* gene, we isolated genomic DNA from 74 F_2 plants (*anl2* × L*er*), digested it with HindIII, and examined it by using DNA gel blot analysis with an *I* element–specific probe. A 7-kb HindIII fragment cosegregated with the *anl2* allele and was considered to be the candidate for the *ANL2* gene into which the *I* element had been inserted. The flanking regions of the *I* elements were amplified by inverse polymerase chain reaction (PCR), and the PCR fragment that hybridized to the 7-kb band was cloned to make an *ANL2*-specific probe. Using this probe, we screened genomic and cDNA libraries. Positive clones were isolated, analyzed, and sequenced. The length of the isolated cDNA clone was 2987 bp, with an open reading frame that predicts a protein of 802 amino acids. Figure 3 shows a physical map of the *ANL2* locus. The total length of genomic DNA sequenced is 9.3 kb. *ANL2* is a complex gene that contains nine exons interrupted by eight introns. The *I* element was inserted 13 bp upstream of the seventh exon.

Using restriction fragment length polymorphism (RFLP) and cleaved amplified polymorphic sequence (CAPS) markers on a population of recombinant inbred (RI) lines of L*er*/Columbia (Col) (Lister and Dean, 1993) and L*er*/Cape Verde Islands (Cvi) (Alonso-Blanco et al., 1998), we were able to map *ANL2* to the top of chromosome 4 located between and closely linked to *mi122* and *g3843*. These data were confirmed by cytogenetical analysis showing that *ANL2* is

Table 1. Amount of Anthocyanin in Rosette Leaves, Stems, and Buds of L*er* and *anl2* Plants and in Young Seeds of *banyuls* (*ban)* and *anl2 ban* Double Mutants

Plant Part	L*er*	*anl2*
Seedling[a]	0.066 ± 0.003[b]	0.042 ± 0.002
Leaves[c]		
Adaxial side	0.39 ± 0.02	0.08 ± 0.01
Abaxial side	0.17 ± 0.01	0.10 ± 0.01
Stems[d]	0.036 ± 0.011	0.013 ± 0.003
Flower buds[e]	0.025 ± 0.007	0.009 ± 0.003
Young seeds in a *ban* background[f]	0.63 ± 0.04	0.68 ± 0.07

[a] Plants were grown for 4 days at 22°C and then for 7 days at 15°C under continuous light (11 W m^{-2}). Anthocyanin was extracted from 10 seedlings by using 1 mL of HCl-methanol. The amount of anthocyanin was expressed as absorbance at 530 nm per seedling. The average of three experiments is shown.

[b] The values indicate ±SE.

[c] Anthocyanin was extracted from each side (adaxial and abaxial) of a rosette leaf separately by using 1 mL of HCl-methanol. The amount of anthocyanin was expressed as absorbance at 530 nm per leaf area. The average of 10 rosette leaves is shown.

[d] Anthocyanin was extracted from five similar stem segments by using 1 mL of HCl-methanol. The value indicates the absorbance at 530 nm per segment. The average of three experiments is shown.

[e] Anthocyanin was extracted from 10 inflorescences by using 1 mL of HCl-methanol. The value indicates the absorbance at 530 nm per inflorescence. The average of three experiments is shown.

[f] Anthocyanin was extracted from young seeds from 10 siliques 7 days after flower opening.

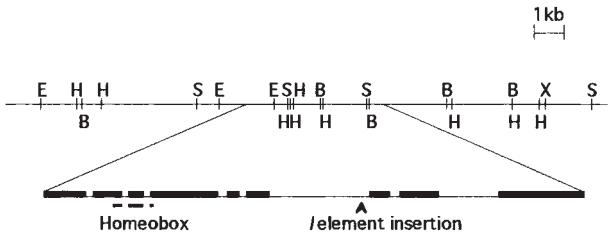

Figure 3. Physical Map of the *ANL2* Locus.

Shown is a physical map of the *ANL2* genomic region. Restriction sites are indicated as follows: B, BamHI; E, EcoRI; H, HindIII; S, SalI; X, XhoI. Closed boxes indicate exons. The position of the *I* element insertion is indicated by an arrowhead.

located on yeast artificial chromosome CIC10C8 (P. Fransz, S. Armstrong, J.H. de Jong, C. van Drunen, P. Zabel, C. Dean, and G. Jones, personal communication). No other locus affecting anthocyanin accumulation has been identified in this region.

Predicted Amino Acid Sequence of ANL2

DNA sequencing showed that the *ANL2* gene encodes a homeodomain protein that belongs to the HD–GL2 group (Figure 4). The homeodomain of ANL2 shares 23 of 29 amino acids that are conserved in >80% of the homeodomain sequences of various organisms (Gehring et al., 1994). Generally, highly conserved amino acids (L-16, F-20, W-48, F-49, N-51, and R-53) are also conserved in ANL2. In a homology search of GenBank, four other proteins—Arabidopsis ATML1 (GenBank accession number U37589), Phalaenopsis ovule-specific protein O39 (Nadeau et al., 1996; GenBank accession number U34743), a Helianthus homeodomain protein (GenBank accession number L76588), and Arabidopsis GL2 (EMBL accession number Z54356)—were found to have a high degree of sequence similarity with ANL2. Among them, ANL2 most resembles ATML1 and O39. Fifty-four percent of the amino acid residues of ATML1 are conserved in ANL2. ANL2 has an extra sequence at the N terminus, and downstream of the homeodomain, there are several regions conserved among the members of the HD–GL2 group. *ANL2* contains two introns in the homeobox region (amino acids 18 and 19 and 57 and 58 of the homeodomain). These intron positions are also conserved in *GL2*.

Nucleotide Sequences of the *I* Element Insertion Site in the Revertants

After crossing the stable mutant with a plant that has only the *En* element in the genome, we observed variegation in the F_2 plants. This shows that the *anl2* mutation is caused by *I* element insertion. We selected several independent stable revertants from progenies of variegated plants and amplified the insertion site of the *I* element by PCR. The sequences of these insertion sites were determined to confirm that we had isolated the *ANL2* gene.

In the *anl2* mutant, the trinucleotide target site sequence (AAG) was duplicated upon insertion of the *I* element. Three types of excision footprints were found in the revertants. Compared with the wild type, two revertants had an addition of 5 bp (CTAAG); another two had an addition of 3 bp (AAG). One revertant had the same sequence as the wild type. All the excision events restored the wild-type phenotype because the *I* element was inserted in intron 6 of the *ANL2* gene.

Expression of *ANL2*

Reverse transcription–PCR (RT-PCR) was performed using primers specific for the sixth and eighth exon sequences (Figures 5A and 5B). A 0.7-kb fragment was amplified in L*er* but not in the stable *anl2* mutant. No signal was detected by DNA gel blot analysis in the *anl2* mutant (data not shown), which means that the *anl2* mutant did not contain any complete *ANL2* mRNA. *ANL2* was expressed in wild-type leaves, stems, buds, and roots. Another primer set designed for the sequence upstream of the *I* element insertion site (specific for the first and fourth exon sequences) gave the same results for both the wild type and the *anl2* mutant (data not shown). This shows that the insertion of the *I* element in the sixth intron does not affect transcription of the *ANL2* gene.

Effect of *ANL2* on Cellular Organization of the Primary Root

Prompted by the fact that the *ANL2* gene is a homeobox gene, we examined morphological aspects of the *anl2* mutant. Cell number and location are invariant in the primary root of Arabidopsis (Dolan et al., 1993). In the primary root of L*er*, an endodermis made up of eight cells is surrounded by a cortex of eight cells and then by an epidermal layer of ~20 cells. The eight hair cell files that stained deeply with toluidine blue overlaid the radial walls of the underlying cortical cells (Figure 6A). The *anl2* mutant had an endodermis made up of eight cells and a cortex of eight cells. However, there were several extra cells between the cortical and epidermal layers (Figure 6B). We call these extra cells intervening cells. The staining pattern of toluidine blue was irregular, and the intervening cells and cortical cells stained similarly. No wild-type plants and no revertant plants had such intervening cells (Table 2). This indicates that the mutation in the *ANL2* gene induced an aberrant arrangement of the cellular organization in the primary root.

The files of hair cells are separated by one or two files of non-hair cells in wild-type plants. In the *anl2* mutant, files of

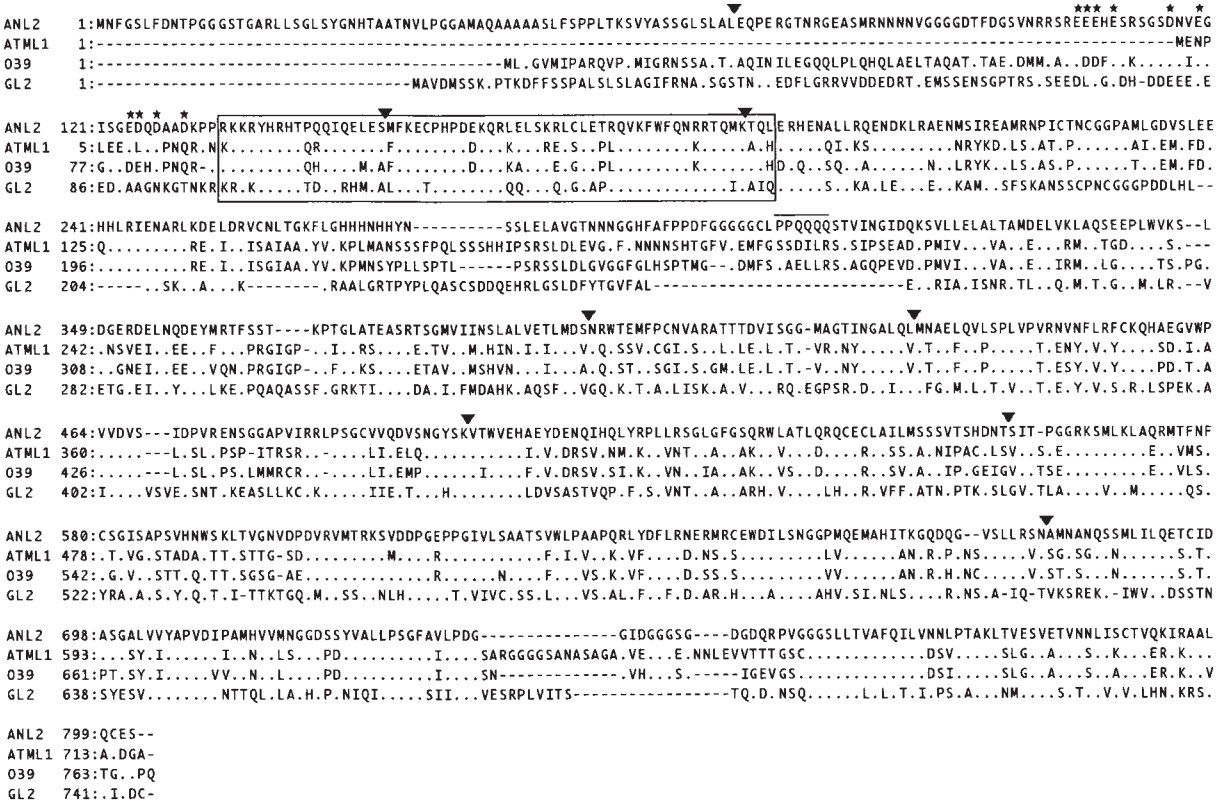

Figure 4. Primary Structure of the ANL2 Protein.

The deduced amino acid sequence of ANL2 (GenBank accession number AF077335) is compared with that of ATML1 (Lu et al., 1996; GenBank accession number U37589) and GL2 (Cristina et al., 1996; EMBL accession number Z54356) from Arabidopsis and O39 (Nadeau et al., 1996; GenBank accession number U34743) from Phalaenopsis. Dots indicate amino acids identical to the ANL2 sequence. Dashes indicate gaps in the sequence to allow for maximal alignment. The homeobox is marked by a box. The arrowheads indicate the position of introns. The stars indicate acidic amino acids. The bar indicates a proline- and glutamine-rich region.

hair cells adjoining each other were sometimes observed (data not shown).

The number of cells in cortical and endodermal layers is invariant in both L*er* and the *anl2* mutant, although the number of cells in the epidermal layer is variable. However, there was no correlation between the number of epidermal cells and the number of intervening cells (Figure 7). This suggests that the intervening cells are formed not by positional shifts of epidermal cells but by abnormal cell divisions.

DISCUSSION

ANL2 Encodes a Homeodomain Protein

In the *En–I* two-element system modified by Aarts et al. (1995), a T-DNA construct carrying an immobilized *En* transposase source activates the transposition of *I* elements, which cause mutations when inserted into a gene. The original *anl2* mutant contained the *En* transposase source and showed variegation of anthocyanin pigmentation in rosette leaves. This phenotype is evidence that the *anl2* mutation is caused by *I* element insertion. DNA gel blot analysis showed that there is one *I* element that cosegregates with the *anl2* mutation. In all revertants, this element was excised from an *anl2*::*I* allele, restoring the *ANL2* transcript. This proves that we have isolated *ANL2*.

The predicted amino acid sequence indicates that *ANL2* codes for a homeodomain protein of the HD–GL2 group. The helix-turn-helix structure and most of the invariant amino acids of the homeodomain (L-16, F-20, W-48, F-49, N-51, and R-53) are conserved in ANL2. There are several motifs that have been implicated in activation of transcription: a proline–glutamine stretch and an acidic region. Therefore, ANL2 probably has DNA binding activity and most likely plays a role as a transcription factor. Within the HD–GL2 group, ANL2 is most similar to the ATML1 protein,

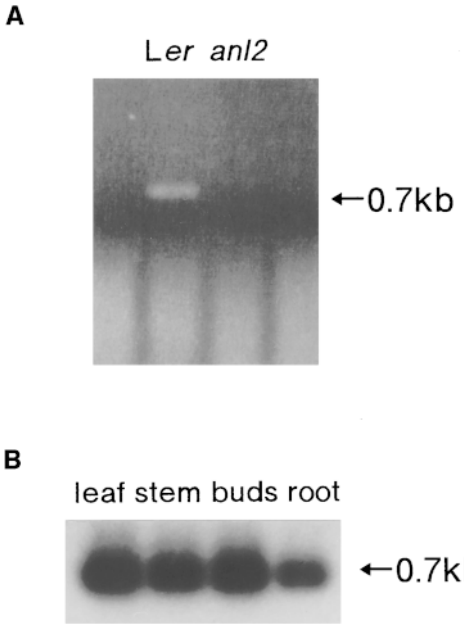

Figure 5. Detection of *ANL2* mRNA by RT-PCR in L*er* and *anl2* Seedlings and Plants.

(A) *ANL2* expression in L*er* and *anl2* seedlings. Total RNA was extracted from 4-day-old L*er* or *anl2* seedlings. The PCR product was detected by ethidium bromide staining after 30 amplification cycles.
(B) *ANL2* expression in leaves, stems, buds, and roots of L*er* plants. Total RNA was extracted from various organs of L*er* plants grown for 3 weeks under continuous light. The PCR product was detected by DNA gel blot analysis after 18 amplification cycles.
Size of the PCR product is shown at right.

which shares several conserved regions downstream of the homeodomain in these two proteins. These regions are conserved for dicots (ANL2 and ATML1) and monocots (O39), suggesting that these regions are important for common processes required for the function of HD–GL2. Despite the similarity in amino acid sequence, *ANL2* showed a different expression pattern from *ATML1*. *ANL2* was expressed in all organs examined, whereas *ATML1* was expressed only in floral buds and siliques (Lu et al., 1996).

Effect on Anthocyanin Accumulation

The mutant allele of *ANL2* had no effect on the pigmentation of seed coat, although it affected the pigmentation of the seedling and mature plant tissues. Thus, the phenotype of the *anl2* mutant was opposite to *tt1*, *tt2*, and *tt8* mutants lacking seed pigment but containing a normal amount of anthocyanin in plant tissues (Koornneef, 1990). This suggests that anthocyanin accumulation in the seed coat is under a different control from that in seedling and mature plant tissues and that *ANL2* is specific for seedling and mature tissues. This suggestion is supported by the experiment using the *anl2 ban* double mutant (Table 1).

In maize, the pattern of anthocyanin pigmentation is determined by the individual members of the two gene families *R*/*B* and *C1*/*Pl*. Pigmentation of kernel requires *R* and *C1*, whereas pigmentation of mature tissues of the plant requires *B* and *Pl* (Mol et al., 1996). It is suggested that *R* and *C1* homologs are involved in anthocyanin biosynthesis of Arabidopsis (Lloyd et al., 1992). These regulatory genes may control the tissue specificity of anthocyanin biosynthesis in Arabidopsis.

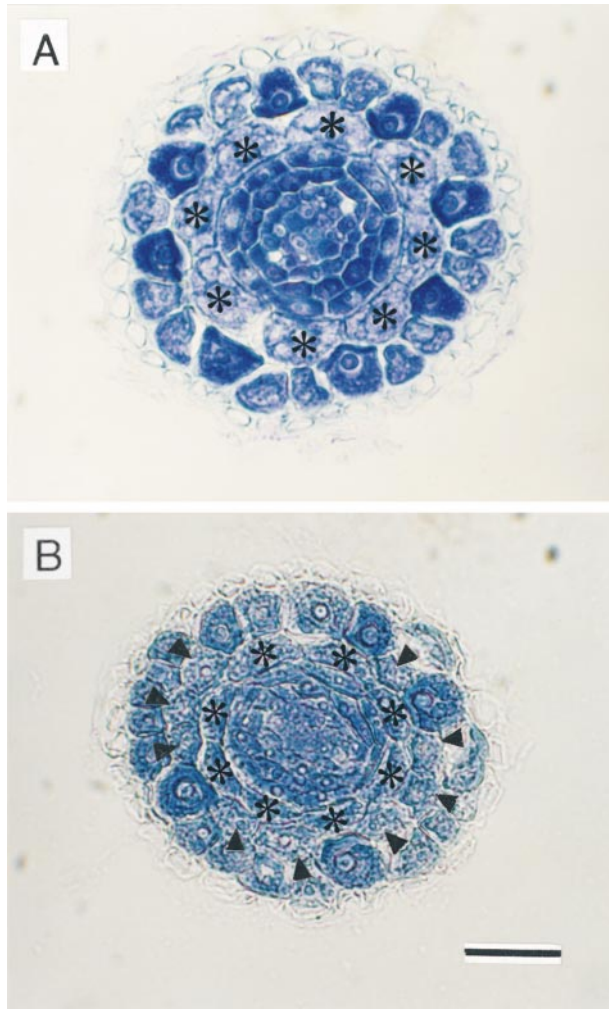

Figure 6. Transverse Sections of the Primary Root of L*er* and *anl2* Plants.

(A) L*er* primary root.
(B) *anl2* primary root.
Asterisks and arrowheads indicate cortical and intervening cells, respectively. Bar in **(B)** = 25 μm for **(A)** and **(B)**.

Table 2. Numbers of Endodermal, Cortical, Intervening, and Epidermal Cells of the Primary Roots of L*er*, *anl2*, and *ANL2* Revertant Plants

Plants	Endodermal Cells	Cortical Cells	Intervening Cells	Epidermal Cells
L*er* (20)[a]	8.0 ± 0[b]	8.0 ± 0.2	0	20.8 ± 1.9
anl2 (21)	7.8 ± 0.6	7.9 ± 0.3	2.2 ± 2.4	18.2 ± 2.6
Revertant (17)	8.1 ± 0.2	8.1 ± 0.3	0	18.8 ± 1.1

[a] Number of roots examined is shown within parentheses.
[b] Values indicate ±SD.

Anthocyanin accumulated in subepidermal tissue on the adaxial side of rosette leaves and in epidermal tissue on the abaxial side of the leaves. There are several observations that the pattern of anthocyanin accumulation in the epidermis is different from that in the subepidermal layer. For example, Parkin (1903) examined tissue localization of anthocyanin in foliage leaves of many species and showed that inducible anthocyanins accumulate in mesophyll but permanent anthocyanins accumulate mainly in epidermis. There is a possibility that *ANL2* is involved in an induction process of anthocyanin synthesis in subepidermal cells. In Arabidopsis, however, both epidermal and subepidermal anthocyanins are similarly induced by light. The effects of other stimuli on the tissue specificity of anthocyanin accumulation remain unknown.

Effect on Cellular Organization

In addition to the reduction in anthocyanin content in leaves, we found that the cellular organization of the primary root was distorted in the *anl2* mutant. This is not surprising, considering that *gl2*, another homeobox gene, also has an effect on both the leaf and root. Several root developmental mutants have been isolated in Arabidopsis (Scheres et al., 1996; Schiefelbein et al., 1997). Some of these mutants have abnormal roots because of excessive cell expansion of a particular tissue (Benfey et al., 1993). Others are root patterning mutants that lack a particular cell layer (Scheres et al., 1995). The *anl2* mutant clearly shows a different phenotype compared with these mutants.

Files of hair cells that adjoined each other were sometimes observed in the *anl2* mutant. This may be caused by the abnormal organization of the root cells. Precise observations regarding the relative positions of the hair cell files and the intervening cells are being made. The intervening cells stained similarly to the cortical cells, but the character of the intervening cells has not been clear. Further studies using epidermis- and cortex-specific reporter genes are required to characterize the intervening cells.

No histological differences were found upon examination of rosette leaf and stem tissues of the *anl2* mutant and the wild type. Because the number and size of cells in these tissues are quite different, depending on the developmental stage, it is possible that we were not able to detect small changes in cellular organization in these tissues. Therefore, we examined cotyledons and hypocotyl tissues but found no differences between L*er* and *anl2* plants. Mutation of *ANL2* apparently does not induce morphological changes in the cotyledons and the hypocotyl, although the accumulation of anthocyanin was affected in these organs.

Function of *ANL2*

A homeodomain protein is generally thought to regulate the transcription of specific target genes (Gehring et al., 1994). Therefore, *ANL2* is unlikely to be a structural gene of anthocyanin biosynthesis. In addition, we found no difference in anthocyanin composition between adaxial and abaxial sides of rosette leaves in wild-type plants by using thin-layer chromatography (data not shown). Thus *ANL2* is probably a regulatory gene that is involved in regulating the tissue-specific accumulation of anthocyanins and in organizing the root.

ANL2 affected anthocyanin accumulation in subepidermal tissues as well as the cellular organization of the primary root. Some regulatory genes are known to affect several independent phenotypes. The *gl2* mutant is defective in trichome development, root hair formation, and mucilage production in the seed coat (Rerie et al., 1994; Masucci et al., 1996). The *ttg* mutant shows not only a morphological

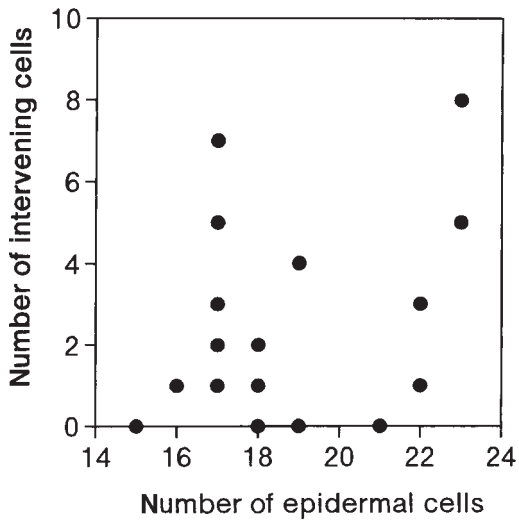

Figure 7. Absence of Correlation between the Number of Epidermal Cells and the Number of Intervening Cells.

The numbers of epidermal cells and intervening cells of the primary root of *anl2* plants were counted under a microscope. Each plot shows the numbers of epidermal cells and intervening cells of one primary root.

defect similar to *gl2* but also is unable to synthesize anthocyanins (Koornneef, 1981). One possibility is that *ANL2* regulates two independent pathways: one is anthocyanin accumulation in subepidermal tissues, and the other is development of cellular organization in the primary root. Another possibility, which is an attractive one, is that *ANL2* determines the identity of subepidermal cells and acts on a developmental process that subsequently interferes with the accumulation of anthocyanin.

METHODS

Plant Material and Growth Conditions

Plant material (*Arabidopsis thaliana*) and normal growth conditions were as described previously (Koornneef et al., 1991). For the experiments in which anthocyanin content was measured, plants were grown on agar plates (5 mM KNO_3, 2.5 mM KH_2PO_4, 2 mM $MgSO_4$, 2 mM $Ca[NO_3]_2$, 0.05 mM Fe-EDTA, micronutrients, 1% sucrose, and 0.8% agar) for 4 days or in soil for 3 weeks at 22°C (7 W m^{-2}) and then at 15°C under continuous white light (11 W m^{-2}) to induce anthocyanin production.

Measurement of Anthocyanin Content

Anthocyanin was extracted from leaves with 1 mL of 0.5 M HCl-methanol at 4°C for 24 hr. To compensate for the absorbance of chlorophyll, we bleached the anthocyanins with H_2O_2, with the difference of $A_{530\,nm}$ before bleaching and after bleaching representing anthocyanin content (Swain and Hillis, 1959). To measure the anthocyanin content of adaxial and abaxial sides separately, we peeled off the epidermis of the abaxial side of a rosette leaf with adhesive tape.

Morphological Observations

For observation of leaf tissue, we embedded fresh tissues in 5% agarose and sliced them with a microslicer (model DTK-1000; Dosaka EM Co., Kyoto, Japan). For observation of the primary root, we fixed seedlings for 4 hr in 50% ethanol, 5% acetic acid, and 3.7% formaldehyde at room temperature, dehydrated them in a graded ethanol series, permeated them with xylene, and then infiltrated them with paraffin. Eight-micrometer sections were made with a microtome and stained with 0.05% toluidine blue. The number of cells was counted under a microscope.

Genomic DNA Isolation and DNA Gel Blot Analysis

Genomic DNA was isolated from three expanded leaves by a downscaled version of a protocol for tomato DNA isolation (Bernatzky and Tanksley, 1986). Total DNA (0.5 to 1 μg) was digested with HindIII, electrophoresed, and transferred to a nylon membrane (Hybond N^+; Amersham) by vacuum blotting (Pharmacia). A 600-bp probe of the left junction of the *Inhibitor* (*I*) element was used to detect restriction fragments containing *I* elements. ^{32}P-labeled probes were made by random prime labeling (Feinberg and Vogelstein, 1984) using α-^{32}P-dATP (110 TBq/mmol; Amersham). After overnight hybridization in 5 × SSC (1 × SSC is 0.15 M NaCl and 0.015 M sodium citrate) and 0.1% SDS at 65°C, we washed the membrane twice with 2 × SSC and 0.1% SDS for 10 min at 65°C before autoradiography.

Reverse Transcription–Polymerase Chain Reaction

The Titan one-tube reverse transcription–polymerase chain reaction (RT-PCR) system (Boehringer Mannheim) was used for RT-PCR. Total RNA was extracted by a standard phenol-SDS extraction method. The same amount of total RNA was used for template, and reactions were performed by using a scaled-down version of the manufacturer's instructions. Two pairs of primers (anl6′ and anl8R′; anl2138′ and anl3320R′) were used to detect the *ANL2* transcript. The sequences of the primers were anl6′ (5′-TTGTCTCCACTGGTTCCGGT-3′), anl8R′ (5′-ATTGGAGCGGAGCAGAGAGA-3′), anl2138′ (5′-ATGAACTTCGGTAGTCTCTT-3′), and anl3320R′ (5′-TGATCAATCCCATTAATCAC-3′). PCR conditions were denaturing at 94°C for 30 sec, annealing at 58°C (anl6′ and anl8R′ primer set) or 50°C (anl2138′ and anl3320R′ primer set) for 30 sec, and extension at 68°C for 90 sec. After 18 cycles (samples for leaves, stems, buds, and roots) or 30 cycles (samples isolated from seedlings of Landsberg *erecta* [L*er*] and *anl2*) of PCR, the products were electrophoresed, transferred to a nylon membrane, and detected by DNA gel blot analysis. ^{32}P-labeled probe was made by using the *ANL2* cDNA as a template.

Screening of cDNA and Genomic Libraries and Sequencing

DNA flanking the *I* element was amplified by inverse PCR, as described previously (Aarts et al., 1995), using HinfI-digested genomic DNA and three sets of nested primers.

The cDNA library that we used, λPRL2, from Columbia (Col) mRNA (Newman et al., 1994), was a gift from the Arabidopsis Biological Resource Center (Columbus, OH) and was constructed in λZipLox (Gibco BRL). Approximately 10^5 plaque-forming units were screened, which resulted in one positive clone of 3 kb. The genomic library was constructed with Sau3AI partially digested genomic DNA from L*er* in λFIX II (Stratagene, La Jolla, CA; C. Alonso-Blanco and A.J.M. Peeters, unpublished data), according to the manufacturer's protocol. Two positive clones (21 and 33) were isolated, and hybridization and restriction analysis showed that these were partially overlapping. Parts of the cDNA were subcloned into pSPORT1 (Gibco BRL) to enable efficient double-strand sequencing, after Taq cycle PCR with SP6 and T7 primers, on an ABI 373 sequencer (Applied Biosystems, Foster City, CA).

Genomic Sequencing

A mapping kit (Stratagene) was used for mapping genomic clones. A 4.6-kb HindIII fragment and a 2.6-kb SalI fragment of phage 21 and a 2.3-kb EcoRI-NotI fragment and a 3.3-kb SalI fragment of phage 33 were subcloned in pBluescript SK+ (Stratagene). A series of deletion fragments to obtain various sizes of deletion clones was made using an ExoIII exonuclease deletion kit (Takara Shuzo, Kyoto, Japan). A DNA sequencer (model 373; Applied Biosystems) was used for sequencing. All cloning procedures were performed with standard methods (Sambrook et al., 1989).

Genetic Mapping of *ANL2*

Mapping was conducted in three separate ways. By using phage 33 as a restriction fragment length polymorphism (RFLP) probe, we identified an EcoRI polymorphism between L*er* and Col. DNA from 96 L*er*/Col recombinant inbred (RI) lines (Lister and Dean, 1993) was isolated, and 400 ng of digested DNA was separated on a 0.7% agarose gel and blotted onto a nylon membrane (Hybond N^+; Amersham). By using ^{32}P-labeled phage 33 as an RFLP probe, we were able to score the genotype of each line, and we calculated the map position by using Joinmap (Stam, 1993). DNA was isolated from L*er*/Cape Verde Islands (Cvi) RI lines constructed in our laboratory (Alonso-Blanco et al., 1998). The sequences of the primers used to amplify the DNA by PCR were anl3p2′ (5′-TATGTAGCGCGAGTAAGCCA-3′) and anl3p3′ (5′-CCATCTTTGACCACTTCCC-3′). Fifty nanograms of genomic DNA was used as a template. The conditions were 35 cycles of denaturing at 94°C for 30 sec, annealing at 56.5°C for 30 sec, and extension at 72°C for 90 sec, using 1 unit of Taq DNA polymerase (Pharmacia) in a total volume of 50 μL and the GeneAmp PCR System 9600 (Perkin Elmer). The DNA amplified from template DNA of ecotypes L*er* and Cvi was digested with several restriction enzymes to identify polymorphic restriction sites. A polymorphism was found for TaqI. The primers were then used to produce a cleaved amplified polymorphic sequence (CAPS) marker on DNA of all the L*er*/Cvi RI lines, which after digestion with TaqI and separation on an agarose gel could be scored. Computer analysis using Joinmap calculated the map position.

Cytogenetical methods using fluorescent in situ hybridization on extended DNA fibers (Fransz et al., 1996) confirmed the outcome of the methods described above (P. Fransz, S. Armstrong, J.H. de Jong, C. van Drunen, P. Zabel, C. Dean, and G. Jones, personal communication).

Analysis of Revertants

Revertants were selected from among the progeny of variegated plants obtained by crossing a stable mutant line and an *Enhancer* (*En*) transposase-containing line. Two primers were designed to amplify a part of the genomic sequence ranging from exons 4 to 7, including the *I* element insertion site. The sequences of the primers used to amplify the DNA by PCR were anl3′ (5′-GTAGCGAGCCATCTTTGAG-3′) and anl4′ (5′-AACCGGTTTAGCTACTGAA-3′). Fifty nanograms of genomic DNA was used as a template. The conditions were 35 cycles of denaturing at 94°C for 30 sec, annealing at 54°C for 30 sec, and extension at 72°C for 60 sec, using 1 unit of Taq DNA polymerase (Pharmacia) in a total volume of 50 μL in a GeneAmp PCR System 9600 (Perkin Elmer). This method produced a single band of 1581 to 1586 bp in all the revertant lines. Each PCR product was directly sequenced using primer anl3′ as sequencing primer.

ACKNOWLEDGMENTS

We thank Dr. Isabera Debeaujon for the gift of *ban* mutant seeds. This work was supported in part by Grants-in-Aid for Scientific Research from the Ministry of Education, Science, and Culture of Japan (Nos. 07740614 and 09640766) and by the European Union BRIDGE/BIOTECH project (No. BIOT-CT90-0207). Tony van Kampen, Dorien Haarsma, Suzanne Hesemans, Mitsuru Futatsugi, and Hirotaka Hayashi are acknowledged for technical assistance. The cDNA library as well as the expressed sequence tag clones were a gift from the Arabidopsis Biological Resource Center, Columbus, OH.

Received October 20, 1998; accepted April 23, 1999.

REFERENCES

Aarts, M.G.M., Dirkse, W., Stiekema, W.J., and Pereira, A. (1993). Transposon tagging of a male sterility gene in *Arabidopsis*. Nature **363,** 715–717.

Aarts, M.G.M., Corzaan, P., Stiekema, W.J., and Pereira, A. (1995). A two-element *Enhancer–Inhibitor* transposon system in *Arabidopsis thaliana*. Mol. Gen. Genet. **247,** 555–564.

Albert, S., Delseny, M., and Devic, M. (1997). *BANYULS*, a novel negative regulator of flavonoid biosynthesis in the *Arabidopsis* seed coat. Plant J. **11,** 289–299.

Alonso-Blanco, C., Peeters, A.J.M., Koornneef, M., Lister, C., Dean, C., van den Bosch, N., Pot, J., and Kuiper, M.T.R. (1998). Development of an AFLP based linkage map of L*er* and Cvi *Arabidopsis thaliana* ecotypes and construction of a L*er*/Cvi recombinant inbred line population. Plant J. **14,** 259–271.

Baima, S., Nobili, F., Sessa, G., Lucchetti, S., Ruberti, I., and Morelli, G. (1995). The expression of the *Athb-8* homeobox gene is restricted to provascular cells in *Arabidopsis thaliana*. Development **121,** 4171–4182.

Bancroft, I., Jones, J.D.G., and Dean, C. (1993). Heterologous transposon tagging of the *DRL1* locus in Arabidopsis. Plant Cell **5,** 631–638.

Beggs, C.J., and Wellmann, E. (1994). Photocontrol of flavonoid biosynthesis. In Photomorphogenesis in Plants, 2nd ed, R.E. Kendrick and G.H.M. Kronenberg, eds (Dordrecht, The Netherlands: Kluwer Academic Publishers), pp. 733–751.

Benfey, P.N., Linstead, P.J., Roberts, K., Schiefelbein, J.W., Hauser, M., and Aeschbacher, R.A. (1993). Root development in *Arabidopsis*: Four mutants with dramatically altered root morphogenesis. Development **119,** 57–70.

Bernatzky, R., and Tanksley, S.D. (1986). Genetics of actin related sequences in tomato. Theor. Appl. Genet. **72,** 314–321.

Blank, F. (1958). Anthocyanins, flavones, xanthones. In Handbuch der Pflanzenphysiologie, Vol. 10, V. Paech and P. Schwarze, eds (Berlin: Springer-Verlag), pp. 300–353.

Cristina, M.D., Sessa, G., Dolan, L., Linstead, P., Baima, S., Ruberti, I., and Morelli, G. (1996). *Arabidopsis* Athb-10 (GLABRA2) is an HD-Zip protein required for regulation of root hair development. Plant J. **10,** 393–402.

de Vetten, N., Quattrocchio, F., Mol, J., and Koes, R. (1997). The *an11* locus controlling flower pigmentation in petunia encodes a novel WD-repeat protein conserved in yeast, plants and animals. Genes Dev. **11,** 1422–1434.

Dolan, L., Janmaat, K., Willemsen, V., Linstead, P., Poethig, S., Roberts, K., and Scheres, B. (1993). Cellular organisation of the *Arabidopsis thaliana* root. Development **119,** 71–84.

Dooner, H.K., and Robbins, T.P. (1991). Genetic and developmental control of anthocyanin biosynthesis. Annu. Rev. Genet. **25,** 173–199.

Feinberg, A.P., and Vogelstein, B. (1984). A technique for radiolabeling DNA restriction endonuclease fragments to specific activity. Addendum. Anal. Biochem. **137,** 266–267.

Fransz, P.F., Alonso-Blanco, C., Liharska, T.B., Peeters, A.J.M., Zabel, P., and Jong, J.H. (1996). High resolution physical mapping in *Arabidopsis thaliana* and tomato by fluorescence in situ hybridization to extended DNA fibers. Plant J. **9,** 421–430.

Gehring, W.J., Affolter, M., and Bürglin, T. (1994). Homeodomain proteins. Annu. Rev. Biochem. **63,** 487–526.

Goodrich, J., Carpenter, R., and Coen, E.S. (1992). A common gene regulates pigmentation pattern in diverse plant species. Cell **68,** 955–964.

Kerstetter, R.A., Laudencia-Chingcuanco, D., Smith, L.G., and Hake, S. (1997). Loss-of-function mutations in the maize homeobox gene, *knotted1*, are defective in shoot meristem maintenance. Development **124,** 3045–3054.

Koornneef, M. (1981). The complex syndrome of *ttg* mutants. Arabidopsis Inf. Serv. **18,** 45–51.

Koornneef, M. (1990). Mutations affecting the testa color in *Arabidopsis*. Arabidopsis Inf. Serv. **27,** 1–4.

Koornneef, M., Hanhart, C.J., and van der Veen, J.H. (1991). A genetic and physiological analysis of late flowering mutants in *Arabidopsis thaliana.* Mol. Gen. Genet. **229,** 57–66.

Lister, C., and Dean, C. (1993). Recombinant inbred lines for mapping RFLP and phenotypic markers in *Arabidopsis thaliana.* Plant J. **4,** 745–750.

Lloyd, A.M., Walbot, V., and Davis, R.W. (1992). *Arabidopsis* and *Nicotiana* anthocyanin production activated by maize regulators *R* and *C1*. Science **258,** 1773–1775.

Long, J.A., Moan, E.I., Medford, J.I., and Barton, M.K. (1996). A member of the Knotted class of homeodomain proteins encoded by the *STM* gene of *Arabidopsis*. Nature **379,** 66–69.

Lu, P., Porat, R., Nadeau, J.A., and O'Neill, S.D. (1996). Identification of a meristem L1 layer–specific gene in Arabidopsis that is expressed during embryonic pattern formation and defines a new class of homeobox genes. Plant Cell **8,** 2155–2168.

Martin, C., and Gerats, T. (1993). The control of flower coloration. In The Molecular Biology of Flowering, B.R. Jordan, ed (Wallingford, UK: CAB International), pp. 219–255.

Martin, C., Prescott, A., Mackay, S., Bartlett, J., and Vrijlandt, E. (1991). Control of anthocyanin biosynthesis in flowers of *Antirrhinum majus*. Plant J. **1,** 37–49.

Masucci, J.D., Rerie, W.G., Foreman, D.R., Zhang, M., Galway, M.E., Marks, M.D., and Schiefelbein, J.W. (1996). The homeobox gene *Glabra 2* is required for position-dependent cell differentiation in the root epidermis of *Arabidopsis thaliana*. Development **122,** 1253–1260.

Mol, J., Jenkins, G., Schäfer, E., and Weiss, D. (1996). Signal perception, transduction, and gene expression involved in anthocyanin biosynthesis. Crit. Rev. Plant Sci. **15,** 525–557.

Nadeau, J.A., Zhang, X.S., Li, J., and O'Neill, S.D. (1996). Ovule development: Identification of stage-specific and tissue-specific cDNAs. Plant Cell **8,** 213–239.

Newman, T., de Bruijn, F.J., Green, P., Keegstra, K., Kende, H., McIntosh, L., Ohlrogge, J., Raikhel, N., Somerville, S., Thomashow, M., Retzel, E., and Somerville, C. (1994). Genes galore: A summary of methods accessing results from large-scale partial sequencing of anonymous *Arabidopsis* cDNA clones. Plant Physiol. **106,** 1241–1255.

Parkin, J. (1903). On the localisation of anthocyan (red cell-sap) in foliage leaves. Rep. Br. Assoc. **73,** 862.

Reiser, L., Modrusan, Z., Margossian, L., Samach, A., Ohad, N., Haughn, G.W., and Fischer, R.L. (1995). The *BELL* gene encodes a homeodomain protein involved in pattern formation in the Arabidopsis ovule primordium. Cell **83,** 735–742.

Rerie, W.G., Feldmann, K.A., and Marks, M.D. (1994). The *GLABRA2* gene encodes a homeodomain protein required for normal trichome development in *Arabidopsis*. Genes Dev. **8,** 1388–1399.

Sambrook, J., Fritsch, E.F., and Maniatis, T. (1989). Molecular Cloning: A Laboratory Manual, 2nd ed. (Cold Spring Harbor, NY: Cold Spring Harbor Laboratory Press).

Scheres, B., Laurenzio, L.D., Willemsen, V., Hauser, M., Janmaat, K., Weisbeek, P., and Benfey, P.N. (1995). Mutations affecting the radial organisation of the *Arabidopsis* root display specific defects throughout the embryonic axis. Development **121,** 53–62.

Scheres, B., McKhann, H.I., and van den Berg, C. (1996). Roots redefined: Anatomical and genetic analysis of root development. Plant Physiol. **111,** 959–964.

Schiefelbein, J.W., Masucci, J.D., and Wang, H. (1997). Building a root: The control of patterning and morphogenesis during root development. Plant Cell **9,** 1089–1098.

Shirley, B.W., Hanley, S., and Goodman, H.M. (1992). Effects of ionizing radiation on a plant genome: Analysis of two Arabidopsis *transparent testa* mutations. Plant Cell **4,** 333–347.

Shirley, B.W., Kubasek, W.L., Storz, G., Bruggemann, E., Koornneef, M., Ausubel, F.M., and Goodman, H.M. (1995). Analysis of *Arabidopsis* mutants deficient in flavonoid biosynthesis. Plant J. **8,** 659–671.

Stam, P. (1993). Construction of integrated linkage maps by means of a new computer package: JOINMAP. Plant J. **3,** 739–744.

Swain, T., and Hillis, H.E. (1959). Phenolic constituents of *Prunus domestica*. I. Quantitative analysis of phenolic constituents. J. Sci. Food Agr. **10,** 63–68.

ANTHOCYANINLESS2, a Homeobox Gene Affecting Anthocyanin Distribution and Root Development in Arabidopsis

Hiroyoshi Kubo, Anton J. M. Peeters, Mark G. M. Aarts, Andy Pereira and Maarten Koornneef

Plant Cell 1999;11;1217-1226
DOI 10.1105/tpc.11.7.1217

This information is current as of October 21, 2020

References	This article cites 34 articles, 15 of which can be accessed free at: /content/11/7/1217.full.html#ref-list-1
Permissions	https://www.copyright.com/ccc/openurl.do?sid=pd_hw1532298X&issn=1532298X&WT.mc_id=pd_hw1532298X
eTOCs	Sign up for eTOCs at: http://www.plantcell.org/cgi/alerts/ctmain
CiteTrack Alerts	Sign up for CiteTrack Alerts at: http://www.plantcell.org/cgi/alerts/ctmain
Subscription Information	Subscription Information for *The Plant Cell* and *Plant Physiology* is available at: http://www.aspb.org/publications/subscriptions.cfm

© American Society of Plant Biologists
ADVANCING THE SCIENCE OF PLANT BIOLOGY